

Primordial magnetic fields from the string network

Kouichirou Horiguchi,^{a,1} Kiyotomo Ichiki,^{a,b} and Naoshi Sugiyama^{a,b,c}

^aDepartment of Physics and Astrophysics, Nagoya University,
Aichi 464-8602, Japan

^bKobayashi-Masukawa Institute for the Origin of Particles and the Universe,
Nagoya University,
Nagoya 464-8602, Japan

^cKavli Institute for the Physics and Mathematics of the Universe (Kavli IPMU), The University of Tokyo,
Chiba 277-8582, Japan

E-mail: horiguchi.kouichirou@h.mbox.nagoya-u.ac.jp, ichiki@a.phys.nagoya-u.ac.jp,
naoshi@nagoya-u.jp

Abstract. Cosmic strings are a type of cosmic defect formed by a symmetry-breaking phase transition in the early universe. Individual strings would have gathered to build a network, and their dynamical motion would induce scalar-, vector- and tensor-type perturbations. In this paper, we focus on the vector mode perturbations arising from the string network based on the one scale model and calculate the time evolution and the power spectrum of the associated magnetic fields. We show that the relative velocity between photon and baryon fluids induced by the string network can generate magnetic fields over a wide range of scales based on standard cosmology. We obtain the magnetic field spectrum before recombination as $a^2 B(k, z) \sim 4 \times 10^{-16} G\mu / ((1+z)/1000)^{4.25} (k/\text{Mpc}^{-1})^{3.5}$ Gauss on super-horizon scales, and $a^2 B(k, z) \sim 2.4 \times 10^{-17} G\mu / ((1+z)/1000)^{3.5} (k/\text{Mpc}^{-1})^{2.5}$ Gauss on sub-horizon scales in co-moving coordinates. This magnetic field grows up to the end of recombination, and has a final amplitude of approximately $B \sim 10^{-17 \sim -18} G\mu$ Gauss at the $k \sim 1 \text{ Mpc}^{-1}$ scale today. This field might serve as a seed for cosmological magnetic fields.

¹Corresponding author.

Contents

1	Introduction	1
2	Model of the strings and their evolution	2
2.1	Wiggly string	2
2.2	Evolution of the string network	4
3	Magnetic fields	5
3.1	Vector mode perturbation	6
3.2	Tight-coupling approximation	7
3.3	Magnetic field generation	8
4	Method	9
5	Result & Discussion	10
5.1	Before recombination	11
5.2	After recombination	12
6	Conclusion	14

1 Introduction

Various observations, such as the cosmic microwave background (CMB) and the dimming of distant supernovae, support the standard big-bang model, which has gained a credible position in modern cosmology in recent years. In standard big-bang cosmology, because of its cooling from a very hot initial state following adiabatic expansion, the universe has experienced a number of phase transitions. These phase transitions are expected to generate topological defects in the universe. The nature of these resulting defects depends on the type of symmetry breaking caused by the phase transitions. For example, the topological defects generated in $\mathcal{O}(N)$ symmetry-breaking phase transitions are called $\mathcal{O}(N)$ global defects and correspond to domain walls, cosmic strings, monopoles, and textures for $\mathcal{O}(N = 1)$, $\mathcal{O}(N = 2)$, $\mathcal{O}(N = 3)$, $\mathcal{O}(N \geq 4)$ symmetry breaking, respectively.

Among others, cosmic strings are expected to affect physics at various scales [1]. There are a number of phenomena caused by cosmic strings, for instance, as gravitational signatures, primordial gravitational waves (PGWs) from cusps and kinks on infinite strings and string loops [2–5], gravitational lensing by strings (strong lensing [6] and microlensing [7]), CMB angular power spectra [8, 9], and so on. As non-gravitational signatures, the following are predicted: ultra-high energy cosmic rays from strings [10] and cusps on string loops via a scalar field [11], and radio bursts from kinks and cusps on strings via the gravitational Aharonov-Bohm effect [12, 13].

Because of the impact on physics, a number of studies exist that aim to place constraints on string tension μ which shows the string energy scale. As for CMB observations, cosmic strings induce CMB anisotropies of the order of $\Delta T/T \sim 4\pi G\mu$, where T is the CMB temperature, ΔT is its fluctuation, and G is the gravitational constant. As a result, the recent CMB temperature measurement by the Planck collaboration provides limits to the energy

scale of cosmic strings [14]. Details of the limits depend on the models of the cosmic strings, for instance, $G\mu \leq 3.2 \times 10^{-7}$ for Abelian Higgs strings and $G\mu \leq 1.5 \times 10^{-7}$ for Nambu-Goto strings [14].

In this paper, we investigate primordial magnetic fields induced by the cosmic string network. Previous works about the generation of primordial magnetic fields from cosmic strings include generation from the motion of wiggly strings [15], shock waves induced by cosmic strings [16, 17], the dynamical friction of strings' motion [18], and via the Harrison mechanism in the early universe [19]. Because of the conservation of vorticity, it is argued that primordial magnetic fields can hardly be produced by cosmic defects [19]. To reassess the generation of primordial magnetic fields from cosmic strings, we focus on the tight coupling relationship between photon and baryon fluids in the early universe and the anisotropic stress of photons. We see that generation of magnetic fields from the cosmic string network is possible if we consider up to second order in the tight coupling expansion including the anisotropic stress of photons. In order to calculate the time evolution of cosmic string networks and their associated magnetic fields, we modified CMBACT [20]; this is the code used to calculate the evolution of the string network and CMB anisotropies from the cosmic string network following the "one scale model" [21–23].

In the next section, we describe the model of the individual strings and the evolution of the string network. In section 3, we investigate magnetic fields generation from the string network by considering the tight coupling approximation between the photon and baryon fluids. In section 4, the method which accounts for the randomness of the strings' initial configuration is given. We then discuss evolution of the magnetic field spectrum before and after the recombination epoch in section 5. Finally, we summarize the features of the magnetic fields from the cosmic string network in section 6. Throughout this paper, we assumed an homogeneous and isotropic expanding universe consistent with the Λ -CDM model as the background metric. We fixed the cosmological parameters to $h = 0.73$, $\Omega_m h^2 = 0.127$, $\Omega_b h^2 = 0.0223$, and $N_\nu = 3.04$, where $H_0 = 100h \text{ km/s/Mpc}$ is the Hubble constant, Ω_m and Ω_b are the density parameters of matter and baryon, and N_ν is the number of massless neutrinos.

2 Model of the strings and their evolution

In this section, we review the evolution of individual strings and the string network. We first introduce the energy–momentum tensor of the individual strings. Moreover, by considering the evolution of the separations, motions, and decays of the strings, we calculate the energy–momentum tensor of the string network. Here we assume a homogeneous and isotropic expanding universe described by the FLRW metric given by

$$ds^2 = a(\tau^2)(d\eta^2 - d\vec{x}^2). \quad (2.1)$$

2.1 Wiggly string

Here we introduce the action and the energy stress tensor of a wiggly cosmic string on the string worldsheet following [8]. We define the string worldsheet (ζ_1, ζ_2) in four dimensional space-time, where $\zeta_1 = \eta$ is the conformal time defined in eq.(2.1). Using these conditions,

we can calculate the action density as

$$S = -\mu \int_{\Sigma} dA \quad (2.2)$$

$$= -\mu \int_{\Sigma} d^2\zeta \left[-\det_{ab}(\gamma^{ab}) \right]^{\frac{1}{2}}, \quad (2.3)$$

where

$$\gamma^{ab} = g_{\mu\nu} \frac{\partial x^\mu}{\partial \zeta_a} \frac{\partial x^\nu}{\partial \zeta_b} \quad (2.4)$$

is the metric on the string worldsheet. Here μ is the string energy density per unit length. From the definition, we can write the energy–stress tensor of the string as

$$T^{\mu\nu} = \frac{\mu}{\sqrt{-g}} \int_{\Sigma} d^2\zeta \left\{ \epsilon \dot{x}^\mu \dot{x}^\nu - \epsilon^{-1} x'^\mu x'^\nu \right\} \delta^{(4)}(y - x(\zeta)), \quad (2.5)$$

with

$$\epsilon = \sqrt{\frac{\dot{x}'^2}{1 - \dot{x}^2}}, \quad (2.6)$$

where dots and primes represent derivatives with respect to the conformal time and ζ_2 , respectively, and we have chosen the gauge as $\dot{x}^\mu x'_\mu = 0$. Following [24], the string tension T and the linear energy density U can be defined by

$$\sqrt{-g} T^{\mu\nu}(y) = \int_{\Sigma} d^2\zeta \sqrt{-\gamma} \{U u^\mu u^\nu - T v^\mu v^\nu\} \delta^{(4)}(y - x(\zeta)), \quad (2.7)$$

where

$$u^\mu u_\mu = -v^\mu v_\mu = 1, \quad u^\mu v_\mu = 0, \quad (2.8)$$

$$(u^\mu v^\rho - v^\mu u^\rho)(u_\rho v_\nu - v_\rho u_\nu) = u^\mu u_\nu - v^\mu v_\nu = \eta_\nu^\mu, \quad (2.9)$$

$$\eta^{\mu\nu} = \gamma^{ab} x'_{,a}{}^\mu x'_{,b}{}^\nu, \quad (2.10)$$

and

$$u^\mu = \frac{\sqrt{\epsilon} \dot{x}^\mu}{(-\gamma)^{1/4}}, \quad v^\mu = \frac{x'^\mu}{\sqrt{\epsilon}(-\gamma)^{1/4}}. \quad (2.11)$$

We can easily check that u^μ and v^μ satisfy eq.(2.8) \sim eq.(2.10). Substituting eq.(2.11) into eq.(2.7) and comparing with eq.(2.5), we can see that

$$U = T = \mu. \quad (2.12)$$

This is the equation of state for a Nambu–Goto string. In practice, in lattice simulations of cosmic strings, the strings are macroscopically straight, but they have wiggles from a microscopic viewpoint [25, 26]. Even though the cosmic strings are macroscopic and straight on the cosmological scale (\sim Mpc), their macroscopic equations of state are affected by the microscopic wiggleness. The equation of state for the wiggly string, smoothing out the small scale structures, is shown in [24, 27]. In this case, we employ effective values of the string tension \tilde{T} and the linear energy density \tilde{U} , with which the equations of states for the wiggly string are denoted as

$$\tilde{T} = \frac{\mu}{\alpha}, \quad \tilde{U} = \alpha\mu. \quad (2.13)$$

Here α is the “wiggleness parameter”, which is a function of time and the string coordinate ζ . The evolution of α is estimated in [8, 25, 28], which show that $\alpha \sim 1.9$ in the radiation dominated era and $\alpha \sim 1.5$ in the matter dominated era. In the late time universe, when the cosmological constant dominates, wiggleness is smoothed out by the exponential expansion of the universe and α becomes equal to unity. Substituting the effective values of eq.(2.13) into eq.(2.7), we can write the effective energy–momentum tensor of a wiggly string $\tilde{T}^{\mu\nu}$ as

$$\tilde{T}^{\mu\nu}(y) = \frac{1}{\sqrt{-g}} \int_{\Sigma} d^2\zeta \sqrt{-\gamma} \left\{ \tilde{U} u^\mu u^\nu - \tilde{T} v^\mu v^\nu \right\} \delta^{(4)}(y - x(\zeta)) \quad (2.14)$$

$$= \frac{\mu}{\sqrt{-g}} \int_{\Sigma} d^2\zeta \left\{ \epsilon \alpha \dot{x}^\mu \dot{x}^\nu - \frac{x'^\mu x'^\nu}{\epsilon \alpha} \right\} \delta^{(4)}(y - x(\zeta)). \quad (2.15)$$

If we consider magnetic field generation by the string network, the wiggleness affects the magnetic field spectrum only through a constant factor α^2 . Here we set $\alpha = 1$ for simplicity, which represents straight strings.

2.2 Evolution of the string network

Following the one-scale model [21–23], the network of cosmic strings can be characterized by a single parameter, the correlation length L , which is defined as

$$L^2 = \frac{\mu}{\rho_{\text{string}}}, \quad (2.16)$$

where ρ_{string} is the energy density of the cosmic string. To simplify the expressions, we introduce the comoving correlation length $l = L/a$. From the energy conservation law and the equation of motion of the string, we can obtain the evolution equations of the string network as [21–23]:

$$\frac{dl}{d\eta} = \mathcal{H} l v^2 + \frac{1}{2} \tilde{c} v, \quad (2.17)$$

$$\frac{dv}{d\eta} = (1 - v^2) \left(\frac{\tilde{k}}{l} - 2\mathcal{H} v \right), \quad (2.18)$$

where $\mathcal{H} = \dot{a}/a$ is the conformal Hubble parameter,

$$v = \sqrt{\frac{\int d\sigma \epsilon \vec{x}^2}{\int d\sigma \epsilon}},$$

is the string’s rms velocity, \tilde{c} is the loop–chopping efficiency,

$$\tilde{k} = \frac{\int d\sigma \epsilon (1 - \vec{x}^2) \vec{x} \cdot \hat{u}}{v(1 - v^2) \int d\sigma \epsilon},$$

is the effective curvature of the strings, and \hat{u} is the unit vector of the curvature radius vector of the string. Here we consider the reduction of the energy density by the expansion of the universe and the decrease of the total length of infinite strings in the Hubble horizon. The total length of infinite strings decreases because infinite strings are chopped due to their collisions, making string loops that immediately decay by radiating gravitational waves from their peakedness [29]. The loop–chopping efficiency \tilde{c} represents the rate at which strings

become loops. In general, \tilde{c} is a function of time as shown in [8, 23]; however its value does not vary much. In the radiation dominated era, $\tilde{c} = c_r = 0.23$, and in the matter dominated era, $\tilde{c} = c_m = 0.18$.

We describe the Fourier transform of the energy–momentum tensor of an individual string as

$$\begin{aligned}\Theta^{\mu\nu}(\vec{k}, \eta) &= \int d^3x e^{i\vec{k}\cdot\vec{x}} T^{\mu\nu}(x) \\ &= \int_{-l/2}^{l/2} d\zeta e^{i\vec{k}\cdot\vec{X}} \left[\epsilon\alpha \dot{X}^\mu \dot{X}^\nu - \frac{X'^\mu X'^\nu}{\epsilon\alpha} \right],\end{aligned}\quad (2.19)$$

where the four vector $X^\mu(\zeta, \eta) = (\eta, \vec{X})$ denotes the coordinates in which the string segment exists. We can represent the vector as

$$X^0 = \eta, \quad \vec{X} = \vec{x}_0 + \zeta \hat{X}' + v\eta \hat{X}, \quad (2.20)$$

where \vec{x}_0 is a random vector that denotes the initial position of the string's mass center, and \hat{X}' and \hat{X} are random unit vectors that fulfill $\hat{X}' \cdot \hat{X} = 0$. In the expression for the energy–momentum tensor of the string, the initial position coordinate \vec{x}_0 appears only as a phase in the inner product with \vec{k} . We can therefore deal with $\vec{k} \cdot \vec{x}_0$ as a random initial phase $\phi_0 : [0, 2\pi]$. Because individual strings have their own initial positions, aligned directions, and velocity directions, we write those of the m -th string as \vec{x}_0^m, \hat{X}'^m and \hat{X}^m . Summing up our description of strings, we obtain the total energy momentum tensor of the string network. Fourier transform of the total energy momentum tensor of the string network $\Theta_{\mu\nu}(\vec{k}, \tau)$ is given by [8],

$$\Theta_{\mu\nu}(\vec{k}, \eta) = \sum_{m=1}^{N_0} \Theta_{\mu\nu}^m(\vec{k}, \eta) T^{\text{off}}(\eta, \eta_m), \quad (2.21)$$

where N_0 is the initial number of the strings, $\Theta_{\mu\nu}^m(\vec{k}, \tau)$ is the energy momentum tensor of the individual strings, η_m is the time of decay for the m -th string, and T^{off} is the smoothing function of the decay. We adopt the functional form of T^{off} from [8, 30] that is given by

$$T^{\text{off}}(\eta, \eta_m) = \begin{cases} 1, & (\eta < f\eta_m) \\ 1/2 + (x^3 - 3x)/4, & (f\eta_m < \eta < \eta_m) \\ 0, & (\eta_m < \eta), \end{cases} \quad (2.22)$$

$$x = 2 \frac{\ln(f\eta_m/\eta)}{\ln f} - 1. \quad (2.23)$$

Here $0 < f < 1$ is a parameter which controls the speed of the strings decay. We fix this value to $f = 0.5$. Considering eq.(2.22) for individual infinite strings, we take account of the decrease in the number of infinite strings by their decay into loops due to their intersections. Because of their random initial positions and directions of motion, the decay time for each string η_m is fixed randomly.

3 Magnetic fields

Infinite strings can be the source of magnetic fields on large scales around the recombination era. In this section, we estimate the amplitude of the magnetic fields produced by the network made of infinite strings.

3.1 Vector mode perturbation

Here we take the Poisson gauge,

$$ds^2 = a^2(\eta)(-(1 + 2\psi)d\eta^2 + 2w_i d\eta dx^i + [(1 - 2\phi)\delta_{ij} + h_{ij}]dx^i dx^j). \quad (3.1)$$

In the same way as [31], using the vector projector tensor

$$\mathcal{O}_{ij}^{(\lambda)}(\hat{k}) = \frac{i\lambda}{\sqrt{2}}(\hat{k}_i e_j^{(\lambda)}(\hat{k}) + \hat{k}_j e_i^{(\lambda)}(\hat{k})), \quad (3.2)$$

we can denote the vector mode part of h_{ij} directly as

$$h_{ij} = \sum_{\lambda=\pm 1} h_V^{(\lambda)} \mathcal{O}_{ij}^{(\lambda)}. \quad (3.3)$$

The evolution equation of the vorticity $\sigma = \dot{h}_V/k$ is given based on the Einstein equation by

$$\dot{\sigma}^{(\lambda)} + 2\mathcal{H}\sigma^{(\lambda)} = 8\pi G a^2 \Pi^{(\lambda)}/k. \quad (3.4)$$

Here $\lambda = \pm$ is the index of polarization, and $\Pi = \Theta_{ij}^{\text{tot}}(k, \tau)\mathcal{O}_{ij}$ is the total anisotropic stress in the vector mode. In this paper, we assume the infinite strings to be the sources of the vector mode perturbations.

In the vector mode, the Euler equation for the baryon fluid is given by

$$\dot{v}_b - \dot{\sigma} + \mathcal{H}(v_b - \sigma) = R\dot{\tau}(v_\gamma - v_b), \quad (3.5)$$

where v_γ and v_b are the velocities of photon and baryon fluids, respectively, ρ_γ and ρ_b are the energy densities of photon and baryon fluids, respectively, $R = 4\rho_\gamma/3\rho_b$ is the photon-baryon ratio, $\dot{\tau} = a\sigma_T n_e$ is the opacity of the Thomson scattering, σ_T is the Thomson scattering cross section, and n_e is the electron number density. The vector mode Boltzmann equations for the photon fluid are given by

$$\dot{v}_\gamma - \dot{\sigma} + \frac{k}{8}\Pi_\gamma = -\dot{\tau}(v_\gamma - v_b), \quad (3.6)$$

$$\dot{\Pi}_\gamma + \frac{8}{5}kI_3 - \frac{8}{5}kv_\gamma = -\dot{\tau}\left(\frac{9}{10}\Pi_\gamma - \frac{9}{5}E_2\right), \quad (3.7)$$

$$\dot{I}_l + k\frac{l}{2l+1}\left(\frac{l+2}{l+1}I_{l+1} - I_{l-1}\right) = -\dot{\tau}I_l \quad (l \geq 3), \quad (3.8)$$

$$\begin{aligned} \dot{E}_l + \frac{(l+3)(l+2)l(l-1)}{(l+1)^3(2l+1)}kE_{l+1} - \frac{l}{2l+1}kE_{l-1} \\ = -\dot{\tau}\left(E_l - \frac{2}{15}\xi\delta_{l2}\right) + \frac{2}{l(l+1)}kB_l, \end{aligned} \quad (3.9)$$

$$\dot{B}_l + \frac{(l+3)(l+2)l(l-1)}{(l+1)^3(2l+1)}kB_{l+1} - \frac{l}{2l+1}kB_{l-1} = -\frac{2}{l(l+1)}kE_l, \quad (3.10)$$

where $\Pi_\gamma = 3I_2$ is the anisotropic stress of the photon fluid, I_l is the l -th order moment of the intensity, E_l and B_l are the l -th order moments of the polarization, and $\xi = 3I_2/4 + 9E_2/2$ [32].

As shown in [31], the topological defects induce v_γ and v_b from the vorticity σ . Then, the relative velocity between the photon and baryon fluids, $v_\gamma - v_b$, plays the main role in exciting the magnetic fields [33, 34]. The evolution of the relative velocity and thus the evolution of the associated magnetic fields are driven by the strength of the coupling between the photon and baryon fluids. Therefore, the magnetic fields evolve differently before and after the epoch of recombination. Before recombination, a tight-coupling approximation can be applied to describe their evolution. However, after recombination, we need to solve the baryon fluid equation eq.(3.5) and the full Boltzmann equations eq.(3.6)~eq.(3.10). We do this numerically.

3.2 Tight-coupling approximation

In the early universe before recombination, photon and baryon fluids are tightly coupled to each other because of the frequent Thomson scattering. In that epoch, the opacity of the Thomson scattering $\dot{\tau}$ was very large and the tight-coupling parameter $k/\dot{\tau}$ takes a very small value ($k/\dot{\tau} \ll 1$). Therefore, we can expand the Boltzmann and the Einstein equations with the tight coupling parameter. This expansion is called the tight-coupling approximation (TCA). In [35], the authors considered magnetic field generation with no external source, and used the first order approximation for the photon's anisotropic stress $\Pi_\gamma^{(1)}$ and the second order approximation for the relative velocity between photon and baryon fluids $v_\gamma^{(2)} - v_b^{(2)}$. In the case where there is an external source, higher order TCA, such as $\Pi_\gamma^{(2)}$ and $v_\gamma^{(3)} - v_b^{(3)}$ are needed [31]. In this paper, we consider the string network as the external source and we need to consider the higher order approximation.

Here we consider the TCA up to the third order in the conformal Newtonian gauge. In the TCA, we expand the relative velocity as $\delta v = v_\gamma - v_b = 0 + \delta v^{(1)} + \delta v^{(2)} + \delta v^{(3)} + \dots$, where $\delta v^{(n)} \propto (k/\dot{\tau})^n$ is the n -th order expansion. Following [31], we find the TCA up to second order for Π_γ and up to third order for δv as,

$$\begin{aligned}\Pi_\gamma^{(1)} &= \frac{32}{15} \left(\frac{k}{\dot{\tau}}\right) v_\gamma^{(0)}, \\ \Pi_\gamma^{(2)} &= \frac{32}{15} \left(\frac{k}{\dot{\tau}}\right) v_\gamma^{(1)} + \frac{176}{45} \left(\frac{k}{\dot{\tau}}\right)^2 \frac{1}{k} \left[\frac{\ddot{\tau}}{\dot{\tau}} v_\gamma^{(0)} - \dot{v}_\gamma^{(0)} \right],\end{aligned}\tag{3.11}$$

$$\delta v^{(1)} = \left(\frac{k}{\dot{\tau}}\right) \frac{\mathcal{H}}{(1+R)k} (v_\gamma^{(0)} - \sigma^{(0)}), \quad (3.12)$$

$$\begin{aligned} \delta v^{(2)} = & \left(\frac{k}{\dot{\tau}}\right) \frac{\mathcal{H}}{(1+R)k} (v_\gamma^{(1)} - \sigma^{(1)}) - \frac{4}{15} \left(\frac{k}{\dot{\tau}}\right)^2 \frac{1}{1+R} v_\gamma^{(0)} \\ & - \left(\frac{k}{\dot{\tau}}\right)^2 \frac{\mathcal{H}(v_\gamma^{(0)} - \sigma^{(0)})}{(1+R)^2 k^2} \left(\frac{\mathcal{H}R}{1+R} + \frac{\dot{\mathcal{H}}}{\mathcal{H}} + \mathcal{H} + \frac{\dot{v}_\gamma^{(0)} - \dot{\sigma}^{(0)}}{v_\gamma^{(0)} - \sigma^{(0)}} - \frac{\ddot{\tau}}{\dot{\tau}} \right), \end{aligned} \quad (3.13)$$

$$\begin{aligned} \delta v^{(3)} = & \left(\frac{k}{\dot{\tau}}\right) \frac{\mathcal{H}}{(1+R)k} (v_\gamma^{(2)} - \sigma^{(2)}) - \frac{4}{15} \left(\frac{k}{\dot{\tau}}\right)^2 \frac{1}{1+R} v_\gamma^{(1)} \\ & - \left(\frac{k}{\dot{\tau}}\right)^2 \frac{\mathcal{H}(v_\gamma^{(1)} - \sigma^{(1)})}{(1+R)^2 k^2} \left(\frac{\mathcal{H}R}{1+R} + \frac{\dot{\mathcal{H}}}{\mathcal{H}} + \mathcal{H} + \frac{\dot{v}_\gamma^{(1)} - \dot{\sigma}^{(1)}}{v_\gamma^{(1)} - \sigma^{(1)}} - \frac{\ddot{\tau}}{\dot{\tau}} \right) \\ & + \frac{4}{15} \left(\frac{k}{\dot{\tau}}\right)^3 \frac{\mathcal{H}}{(1+R)^2 k} v_\gamma^{(0)} \\ & - \frac{2}{45k} \left(\frac{k}{\dot{\tau}}\right)^3 \frac{1}{(1+R)^2} \left[(23+11R) \frac{\ddot{\tau}}{\dot{\tau}} v_\gamma^{(0)} - (17+11R) \dot{v}_\gamma^{(0)} - \frac{6v_\gamma^{(0)} \mathcal{H}R}{1+R} \right]. \end{aligned} \quad (3.14)$$

In this paper, we assume that the strings are the only source of vorticity. In this case, the fact that $v^{(0)} = \sigma^{(0)}$ plays the most important role. Because of this, the first order TCA of the relative velocity is given as $\delta v^{(1)} = 0$. Therefore, $\delta v^{(2)} \sim (k/\dot{\tau})^2 \sigma/(1+R)$ is the leading order of the TCA. In our numerical calculation, evolution equations are switched from the TCA to the full Boltzmann equations at the epoch of recombination. At this time, we need to calculate an accurate relative velocity $\delta v^{(2)} = v_\gamma^{(2)} - v_b^{(2)}$ via the Boltzmann equations. The junction conditions for $v_\gamma^{(2)}$ and $v_b^{(2)}$ at recombination are given by the following equations,

$$\dot{v}_b^{(2)} - \dot{\sigma}^{(2)} + \mathcal{H}(v_b^{(2)} - \sigma^{(2)}) = R\dot{\tau} \delta v_{\text{TCA}}^{(3)}, \quad (3.15)$$

$$\dot{v}_\gamma^{(2)} - \dot{\sigma}^{(2)} + \frac{k}{8} \Pi_\gamma^{(2)} = -\dot{\tau} \delta v_{\text{TCA}}^{(3)}. \quad (3.16)$$

Therefore we need $\delta v^{(3)}$ for an accurate calculation of $\delta v^{(2)}$ at the switching time [31] from the TCA to the full Boltzmann equations.

3.3 Magnetic field generation

The relative velocity between the photon and baryon fluids can induce magnetic fields [33, 34]. In the early universe, electrons move together with photons because of the frequent Thomson scattering. Because this scattering separates electrons from photons, electric fields are induced and their rotations generate magnetic fields via the Maxwell equations. The evolution equation of the magnetic fields is given by [33, 34, 36],

$$\frac{1}{a} \frac{d}{d\eta} (a^2 B^i) = \frac{4\sigma_T \rho_\gamma a}{3e} \epsilon^{ijk} \partial_k (v_{\gamma j} - v_{b j}), \quad (3.17)$$

where e is the elementary charge and ϵ^{ijk} is the Levi-Civita tensor. We can obtain the magnetic field spectrum by integrating eq.(3.17) in Fourier space as

$$\begin{aligned} \left\langle a^4 B^i(\vec{k}, \eta) B_i^*(\vec{k}', \eta) \right\rangle = & \left(\frac{4\sigma_T}{3e} \right)^2 (\delta^{jl} \delta^{km} - \delta^{jm} \delta^{kl}) k_k k'_m \left\langle \int_0^\eta d\eta' a^2(\eta') \rho_\gamma(\eta') \delta v_j(\vec{k}, \eta') \right. \\ & \left. \times \int_0^\eta d\eta'' a^2(\eta'') \rho_\gamma(\eta'') \delta v_l^*(\vec{k}', \eta'') \right\rangle. \end{aligned} \quad (3.18)$$

The ensemble average of the relative velocity can be written as

$$\langle \delta v_j(\vec{k}, \eta') \delta v_l^*(\vec{k}', \eta'') \rangle = P_{jl}(\hat{k}) \delta v(k, \eta') \delta v(k, \eta'') (2\pi)^3 \delta(\vec{k} - \vec{k}'), \quad (3.19)$$

$$P_{jl}(\hat{k}) = \delta_{jl} - \hat{k}_j \hat{k}_l. \quad (3.20)$$

Substituting eq.(3.19) and eq.(3.20) into eq.(3.18), we obtain the correlation function of the magnetic fields as [35]

$$\langle B^i(\vec{k}, \eta) B_i(\vec{k}', \eta) \rangle = (2\pi)^3 S_B(k, \eta) \delta^{(3)}(\vec{k} - \vec{k}'), \quad (3.21)$$

where

$$a^4(\eta) \frac{k^3}{2\pi^2} S_B(k, \eta) = 2 \frac{k^3}{2\pi^2} \left(\frac{4\sigma_T}{3e} \right)^2 k^2 \left[\int_0^\eta d\eta' a^2(\eta') \rho_\gamma(\eta') \delta v(k, \eta') \right]^2. \quad (3.22)$$

The source of this spectrum is δv , which is driven by σ .

4 Method

Once the initial configuration of the string network and its evolution are fixed, the spectrum of the magnetic fields can be calculated as shown in section 3.

However, the string network has a random initial configuration, and individual strings decay at random. To see the statistical properties of the generated magnetic fields, we need to average out their randomness. For that, we prepare a number of realizations for the string network and calculate the power spectrum eq.(3.22) under each realization.

In practice, we realize the magnetic fields by repeatedly following the three steps listed below using CMBACT[20]:

1. Set a random initial configuration of the string network.
2. Compute the evolution of the energy–momentum tensor of the string network by considering random decay of the strings.
3. Calculate the magnetic field spectrum.

In the m -th realization, the m -th power spectrum $S_B^m(k, \eta)$ in eq.(3.21) is calculated. Moreover, we can obtain the averaged power spectrum $S_B^{\text{ave}}(k, \eta)$ as

$$S_B^{\text{ave}}(k, \eta) = \frac{1}{N_r} \sum_{m=1}^{N_r} S_B^m(k, \eta), \quad (4.1)$$

where N_r is the number of realizations, and we fix $N_r = 100$ in this paper. Because each S_B^m has an initial configuration and evolution, the averaged power spectrum, $S_B^{\text{ave}}(k, \eta)$, can not be divided into an initial power spectrum and common transfer functions. Therefore, to see the statistical properties of the generated magnetic fields, we need to calculate a number of spectra under different realizations and average them out as eq.(4.1).

According to the above argument and calculating eq.(3.22) numerically, we can obtain the power spectrum of the magnetic fields from the string network as shown in figure 1 and figure 2. Figure 1 shows magnetic field spectra before recombination when the TCA can be applied, whereas figure 2 shows the spectra after recombination when the TCA is invalid.

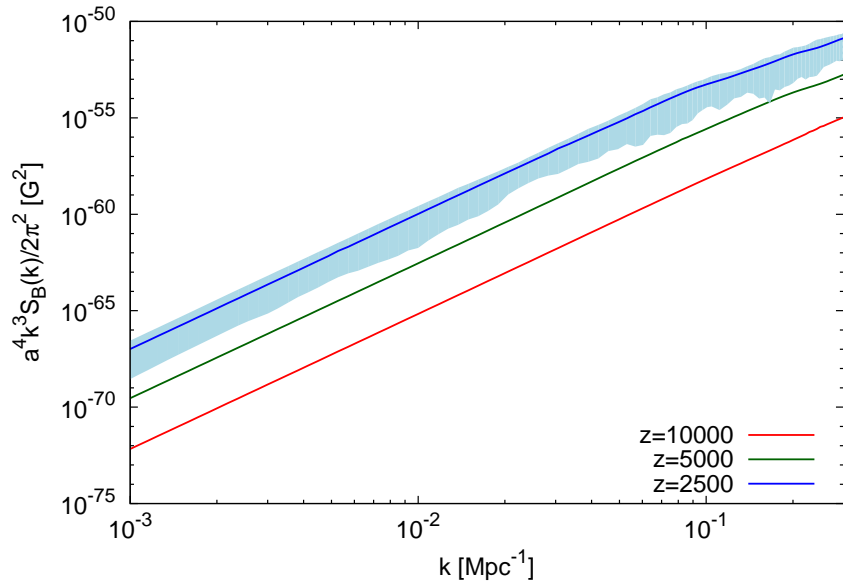


Figure 1. Power spectra of magnetic fields at $z = 10,000$ (red solid line), $5,000$ (green solid line), and $2,500$ (blue solid line) from the infinite string network with $G\mu = 1.1 \times 10^{-6}$. We averaged 100 realizations and the light-blue region is the 68% confidence interval for the $z = 2,500$ case. Under these redshifts, the TCA is valid.

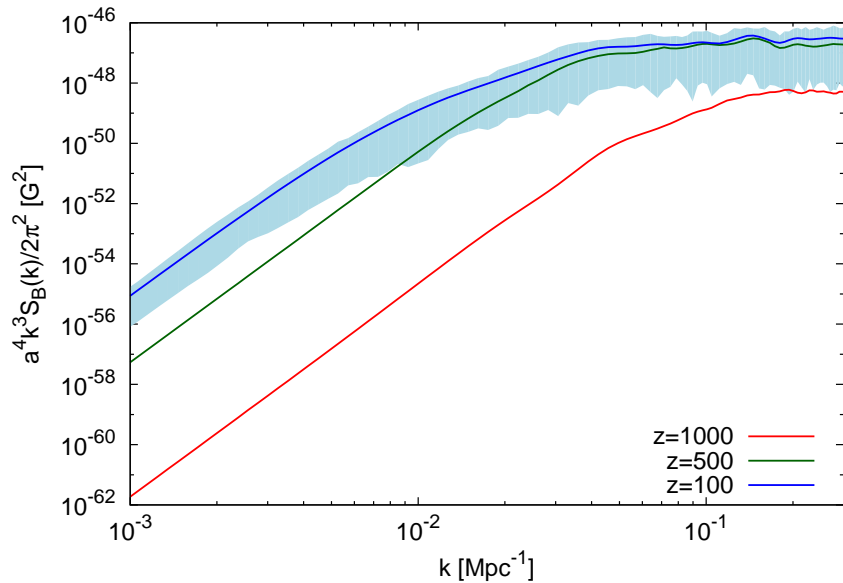


Figure 2. Same as figure 1, but at $z = 1,000, 500, 100$. In these epochs, the TCA is invalid.

5 Result & Discussion

In this section, we will give an analytical interpretation of the magnetic field spectrum arising from the string network. Here to understand the behavior of the spectrum, we investigate

the evolution of magnetic fields separately before and after recombination.

5.1 Before recombination

Before recombination, Thomson scattering between photons and electrons occurs frequently; therefore, we can use the TCA. Focusing on the vector mode that is responsible for the generation of magnetic fields, all of the perturbations are induced by vorticity σ from the string network. This assumption leads the first order TCA of the relative velocity to be zero $\delta v^{(1)} = 0$; therefore, the second order TCA of the relative velocity $\delta v^{(2)}$ is the leading order of δv [31],

$$\delta v \approx \delta v^{(2)} \propto \left(\frac{k}{\dot{\tau}}\right)^2 \frac{v_\gamma^{(0)}}{1+R} = \left(\frac{k}{\dot{\tau}}\right)^2 \frac{\sigma^{(0)}}{1+R} = \begin{cases} k^2 a^5 \sigma^{(0)} & (\text{for rad. dominated era}) \\ k^2 a^4 \sigma^{(0)} & (\text{for mat. dominated era}). \end{cases} \quad (5.1)$$

Sourced by this relative velocity, magnetic fields are generated via eq.(3.22) in individual realizations. Here we define the source function of the magnetic fields $F_s(k, \eta)$ as

$$F_s(k, \eta) \equiv \int_0^\eta d\eta' a^2(\eta') \rho_\gamma(\eta') \delta v(k, \eta'). \quad (5.2)$$

Assuming $\sigma \propto a^\nu$, and integrating eq.(3.4), we can find $\nu \geq -2$ once the anisotropic stress Π from the string network arises. Then, substituting $\sigma \propto a^\nu$ and eq.(5.1) into eq.(5.2), we find that the source function $F_s(k, \eta)$ always increases with time. This means that the co-moving magnetic fields induced in this era are always increasing.

Following the above argument, we obtain a spectrum of the magnetic fields $S_B^m(k, \eta)$, which grows in time for each realization. Averaging these spectra in the manner explained in section 4, we calculate the averaged magnetic field power spectrum as shown in figure 1. From figure 1, we can find approximate expressions for the magnetic field spectrum. On super-horizon scales, the expression is given by

$$a^4(\eta) \frac{k^3}{2\pi^2} S_B(k, z) \approx 1.6 \times 10^{-31} (G\mu)^2 \left(\frac{1+z}{1000}\right)^{-8.5} \left(\frac{k}{\text{Mpc}^{-1}}\right)^7 [\text{G}^2], \quad (5.3)$$

and on sub-horizon scales,

$$a^4(\eta) \frac{k^3}{2\pi^2} S_B(k, z) \approx 5.8 \times 10^{-34} (G\mu)^2 \left(\frac{1+z}{1000}\right)^{-7} \left(\frac{k}{\text{Mpc}^{-1}}\right)^5 [\text{G}^2]. \quad (5.4)$$

On super horizon scales, we find that the wavenumber dependence is the same as that of the magnetic field spectrum from texture [31] and second order density perturbations [36, 37], but slightly different from the magnetic fields generated in Einstein-aether gravity $\langle B_{\text{EA}}^2(k) \rangle \propto k^8$ [38]. The power spectrum of anisotropic stress arising from the string network is shown in figure 3. On sub-horizon scales, we find the power spectrum of magnetic fields as $k^3 S_B(k) \propto k^5$. To understand this scale dependence, we show the power spectrum of anisotropic stress arising from the string network in figure 3.3. On sub-horizon scales, the spectrum shows $\Pi \propto k^{-1}$. From the equations eq.(3.4) and eq.(3.13) we find the relations $\sigma \propto \Pi/k$ and $\delta v \propto k^2 \sigma$, which imply that $k^3 S_B(k) \propto k^5$ from eq.(3.22). The wavenumber dependence differs from the other models which are given by $\langle B_{\text{NLMS}}^2(k) \rangle \propto k^1$ [31], $\langle B_{\text{rec}}^2(k) \rangle \propto k^2$ or $k^{2/3}$ [36] and $\langle B_{\text{EA}}^2(k) \rangle \propto k^2$ or k^{-2} [38].

On smaller scales before recombination, δv begins to decay at the Silk damping scale. Here, the co-moving spectrum can be written as eq.(5.14) $\langle a^4 B^2(k, a) \rangle \propto k^5 a^{-7}$ and the Silk

scale can be written as $k_{\text{Silk}} \propto a^{-3/2}$ [39]. In the same way as [40], we obtain the power spectrum of magnetic fields at scales smaller than the Silk scale as $\langle a^4 B_{\text{Silk}}^2(k) \rangle \propto k^{1/3}$. This spectrum continues to the horizon scale of electron positron pair annihilation, $k \sim 10^5 \text{Mpc}^{-1}$, where the mechanism of magnetic field generation considered in this paper ceases to function [40].

5.2 After recombination

Because the TCA was valid before recombination, we only needed the expression of δv up to $\delta v^{(2)}$ for the source of the magnetic fields. However, around recombination, as the number density of free electrons decreases, the frequency of the Thomson scattering between photons and electrons decreases. Moreover the photons and electrons gradually decouple. Then, the baryon fluid becomes less able to catch up with photon fluid and the TCA breaks down. After this switching epoch, to obtain δv , we need to calculate the full Boltzmann-Einstein system eq.(3.4)~eq.(3.10). In general, it is difficult to solve the Boltzmann equations and see the evolution of δv analytically. However, on super-horizon scales, we can estimate δv using the condition $k\eta \ll 1$. By integrating eq.(3.5) and eq.(3.6), baryon and photon fluids velocities can be denoted as

$$v_b(k, \eta) = \sigma(k, \eta) + \frac{1}{a(\eta)} \int^\eta d\eta' a(\eta') \dot{\tau}(\eta') R(\eta') \delta v(k, \eta') \quad (5.5)$$

$$= \sigma(k, \eta) + R(\eta) \int^\eta d\eta' \dot{\tau}(\eta') \delta v(k, \eta'), \quad (5.6)$$

$$v_\gamma(k, \eta) = \sigma(k, \eta) - \frac{k}{8} \int^\eta d\eta' \Pi_\gamma(k, \eta') - \int^\eta d\eta' \dot{\tau}(\eta') \delta v(k, \eta'). \quad (5.7)$$

From eq.(5.5)–eq.(5.7), we obtain the differential equation for δv ,

$$\dot{\delta v} \simeq -\frac{k}{8} \Pi_\gamma(k, \eta) - \dot{\tau}(\eta) \delta v(k, \eta'), \quad (5.8)$$

where we neglected the second term on the RHS of eq.(5.5) since $R(\eta) = 4\rho_\gamma/3\rho_b \ll 1$ after recombination. We solve it to obtain the form of $\delta v(k, \eta)$

$$\delta v(k, \eta) \simeq -\frac{k}{8} e^{-\tau(\eta)} \int^\eta d\eta' \Pi_\gamma(k, \eta') e^{\tau(\eta')}. \quad (5.9)$$

Writing the anisotropic stress of photons from eq.(3.7) as,

$$\Pi_\gamma(k\eta) \sim \frac{8}{5} k \int^\eta d\eta' v_\gamma(k, \eta'), \quad (5.10)$$

we can estimate δv using v_γ as

$$\delta v(k, \eta) \sim -k^2 e^{-\tau(\eta)} \int^\eta d\eta' e^{\tau(\eta')} \int^{\eta'} d\eta'' v_\gamma(k, \eta''). \quad (5.11)$$

Substituting eq.(5.10) and eq.(5.11) into eq.(5.7), we can see that $v_\gamma(k, \eta) = \sigma(k, \eta) + \mathcal{O}((k\eta)^2)$. Because of this, δv on super-horizon scales should be

$$\delta v(k, \eta) \sim -k^2 e^{-\tau(\eta)} \int^\eta d\eta' e^{\tau(\eta')} \int^{\eta'} d\eta'' \sigma(k, \eta''). \quad (5.12)$$

After vorticity σ becomes source free, σ evolves as $\sigma \propto a^{-2}$ and the source function eq.(5.2) becomes constant. Then, the evolution of the magnetic fields finishes at super-horizon scales.

On sub-horizon scales, the same argument as that for the super-horizon holds true, and we can see the same relationship between δv and v_γ as in eq.(5.11). The main difference in this case is the effects of the higher order terms in $k\eta$. On sub-horizon scales ($k\eta \geq 1$), the photon fluid velocity v_γ evolves following not the first but the second and third terms on the RHS of eq.(5.7) (higher order terms in $k\eta$). Subsequently, after the recombination epoch, the third term vanishes and the evolution of v_γ follows the free-streaming solution. Then, the conformal time dependence of eq.(5.11) is up to $\delta v \propto \eta^2$, and the generation of magnetic fields finishes.

In each realization, magnetic fields are induced by this mechanism. As before, because the evolution of magnetic fields varies in realizations, we need to take the realization average as in section 4. The averaged magnetic field power spectrum after recombination is given in figure 2. We can see that the anisotropic stress induced by the string network is independent of the wavenumber k on the super-horizon scale from figure 3. Using eq.(3.4), eq.(3.22) and eq.(5.12), the wavenumber power on the super-horizon scale is the same as that before recombination, $\langle B^2(k) \rangle \propto k^7$. The expression of the magnetic field spectrum today can be written as

$$a^4(\eta) \frac{k^3}{2\pi^2} S_B(k, z) \approx 7 \times 10^{-23} (G\mu)^2 \left(\frac{k}{\text{Mpc}^{-1}} \right)^7 \quad [\text{G}^2], \quad (5.13)$$

on super-horizon scales and,

$$a^4(\eta) \frac{k^3}{2\pi^2} S_B(k, z) \approx 2.5 \times 10^{-35} (G\mu)^2 \quad [\text{G}^2], \quad (5.14)$$

on sub-horizon scales at $z = 100$ as shown in figure 2.

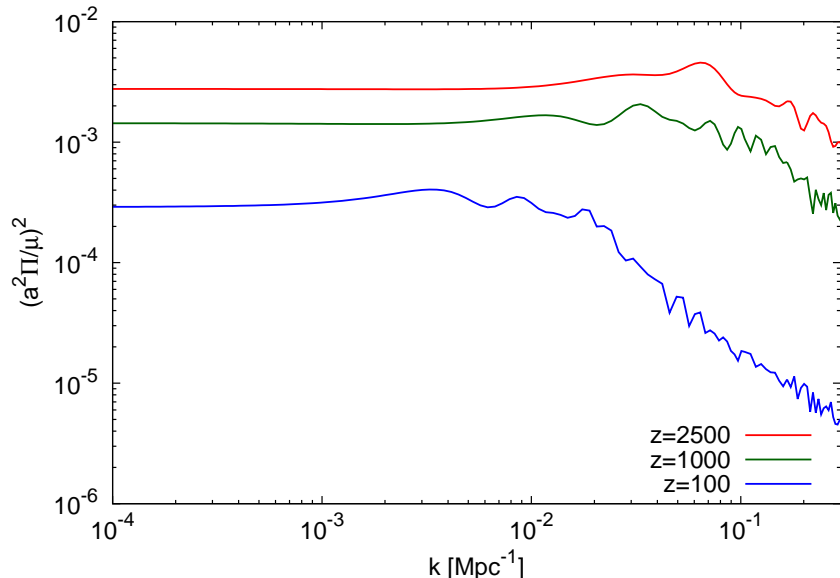


Figure 3. Wavenumber dependence of the anisotropic stress at $z = 2500$ (red solid line), 1000 (green solid line), 100 (blue solid line) from the infinite string network.

Finally let us discuss implications of these magnetic fields. If such magnetic fields existed in the early universe, strong magnetic amplification would occur in the accretion shocks of primordial gases during structure formation of the universe. Then they could provide extra pressure and suppress the fragmentation of gas clumps, supporting the formation of massive protostars and super massive black holes [41]. Moreover, they would affect the hyperfine structure of neutral hydrogens in primordial gases and might be observed via the anisotropic power spectrum of the brightness temperature of the 21-cm line with future surveys as discussed in [42].

6 Conclusion

In this paper, we estimated the magnetic field spectrum from the cosmic string network. First, we calculated the evolution of the cosmic string network under the process of the one scale model and its energy momentum tensor using CMBACT [20]. Then, we solved the Boltzmann-Einstein system to obtain the relative velocity between the photon and baryon fluids using the tight coupling approximation and saw that the leading order of TCA for δv was $\mathcal{O}((k/\dot{\tau})^2)\sigma$ before recombination. Finally, we obtained the power spectrum of the magnetic fields via eq.(3.22), before recombination, as $a^2\sqrt{B^2(k, z)} \sim 4 \times 10^{-16} G\mu/((1+z)/1000)^{4.25} (k/\text{Mpc}^{-1})^{3.5}$ Gauss on super-horizon scales, and $a^2\sqrt{B^2(k, z)} \sim 2.4 \times 10^{-17} G\mu/((1+z)/1000)^{3.5} (k/\text{Mpc}^{-1})^{2.5}$ Gauss on sub-horizon scales in co-moving coordinates. On scales smaller than the Silk damping scale, the spectrum could be calculated as $a^2\sqrt{B^2(k)} \propto k^{1/6}$. After recombination, the spectrum was driven by the evolution of vorticity on super-horizon scales and the coupling between photon and baryon fluids on sub-horizon scales. When the recombination epoch came to an end, the evolution of magnetic fields also ceased. The magnetic field spectrum today is $a^2\sqrt{B^2(k, z)} \sim 2 \times 10^{-11} G\mu (k/\text{Mpc}^{-1})^{3.5}$ Gauss on super-horizon scales and $a^2\sqrt{B^2(k, z)} \sim 5 \times 10^{-17} G\mu$ Gauss on sub-horizon scales.

Acknowledgement

This work is supported in part by a Grant-in-Aid for JSPS Research under Grant No.15J05029 (K.H.) and a Grant-in-Aid for JSPS Grant-in-Aid for Scientific Research under Grant No. 24340048 (K.I.), 25287057 (N.S.) and 15H05890 (N.S.).

References

- [1] T. Vachaspati, L. Pogosian, and D. Steer, *Cosmic Strings*, ArXiv e-prints (June, 2015) [[arXiv:1506.0403](#)].
- [2] T. Damour and A. Vilenkin, *Gravitational Wave Bursts from Cosmic Strings*, Physical Review Letters **85** (Oct., 2000) 3761, [[gr-qc/0004075](#)].
- [3] S. Kuroyanagi, K. Miyamoto, T. Sekiguchi, K. Takahashi, and J. Silk, *Forecast constraints on cosmic string parameters from gravitational wave direct detection experiments*, Phys. Rev. D **86** (July, 2012) 023503, [[arXiv:1202.3032](#)].
- [4] J. J. Blanco-Pillado, K. D. Olum, and B. Shlaer, *Number of cosmic string loops*, Phys. Rev. D **89** (Jan., 2014) 023512, [[arXiv:1309.6637](#)].
- [5] M. Kawasaki, K. Miyamoto, and K. Nakayama, *Gravitational waves from kinks on infinite cosmic strings*, Phys. Rev. D **81** (May, 2010) 103523, [[arXiv:1002.0652](#)].

- [6] K. J. Mack, D. H. Wesley, and L. J. King, *Observing cosmic string loops with gravitational lensing surveys*, Phys. Rev. D **76** (Dec., 2007) 123515, [[astro-ph/0702648](#)].
- [7] K. Kuijken, X. Siemens, and T. Vachaspati, *Microlensing by cosmic strings*, MNRAS **384** (Feb., 2008) 161–164, [[arXiv:0707.2971](#)].
- [8] L. Pogosian and T. Vachaspati, *Cosmic microwave background anisotropy from wiggly strings*, prd **60** (Oct., 1999) 083504, [[astro-ph/9903361](#)].
- [9] A. Avgoustidis, E. J. Copeland, A. Moss, and D. Skliros, *Fast analytic computation of cosmic string power spectra*, Phys. Rev. D **86** (Dec., 2012) 123513, [[arXiv:1209.2461](#)].
- [10] P. Bhattacharjee, *Origin and propagation of extremely high energy cosmic rays*, Phys. Rep. **327** (Mar., 2000) 109–247, [[astro-ph/9811011](#)].
- [11] T. Vachaspati, *Cosmic rays from cosmic strings with condensates*, Phys. Rev. D **81** (Feb., 2010) 043531, [[arXiv:0911.2655](#)].
- [12] K. Jones-Smith, H. Mathur, and T. Vachaspati, *Aharonov-Bohm radiation*, Phys. Rev. D **81** (Feb., 2010) 043503, [[arXiv:0911.0682](#)].
- [13] D. A. Steer and T. Vachaspati, *Light from cosmic strings*, Phys. Rev. D **83** (Feb., 2011) 043528, [[arXiv:1012.1998](#)].
- [14] Planck Collaboration, P. A. R. Ade, N. Aghanim, C. Armitage-Caplan, M. Arnaud, M. Ashdown, F. Atrio-Barandela, J. Aumont, C. Baccigalupi, A. J. Banday, and et al., *Planck 2013 results. XXV. Searches for cosmic strings and other topological defects*, A&A **571** (Nov., 2014) A25, [[arXiv:1303.5085](#)].
- [15] T. Vachaspati and A. Vilenkin, *Large-scale structure from wiggly cosmic strings*, Phys. Rev. Lett. **67** (Aug, 1991) 1057–1061.
- [16] D. N. Vollick, *Cosmic string shocks, magnetic fields, and microwave anisotropies*, Phys. Rev. D **48** (Oct, 1993) 3585–3591.
- [17] T. Vachaspati, *Structure of wiggly-cosmic-string wakes*, Phys. Rev. D **45** (May, 1992) 3487–3496.
- [18] P. P. Avelino and E. P. S. Shellard, *Dynamical friction on cosmic string motion and magnetic field generation*, Phys. Rev. D **51** (May, 1995) 5946–5949.
- [19] L. Hollenstein, C. Caprini, R. Crittenden, and R. Maartens, *Challenges for creating magnetic fields by cosmic defects*, Phys. Rev. D **77** (Mar., 2008) 063517, [[arXiv:0712.1667](#)].
- [20] “<http://www.sfu.ca/~levon/cmbact.html>.”
- [21] T. W. B. Kibble, *Evolution of a system of cosmic strings*, Nuclear Physics B **252** (1985) 227–244.
- [22] D. P. Bennett, *Evolution of cosmic strings. ii*, Phys. Rev. D **34** (Dec, 1986) 3592–3607.
- [23] C. Martins and E. Shellard, *Quantitative string evolution*, Phys.Rev. **D54** (1996) 2535–2556, [[hep-ph/9602271](#)].
- [24] B. Carter, *Integrable equation of state for noisy cosmic string*, Phys. Rev. D **41** (Jun, 1990) 3869–3872.
- [25] D. P. Bennett and F. m. c. R. Bouchet, *High-resolution simulations of cosmic-string evolution. i. network evolution*, Phys. Rev. D **41** (Apr, 1990) 2408–2433.
- [26] G. Gibbons, S. Hawking, and T. Vachaspati, The Formation and evolution of cosmic strings. Cambridge University Press, 1990.
- [27] A. Vilenkin, *Effect of small-scale structure on the dynamics of cosmic strings*, Phys. Rev. D **41** (May, 1990) 3038–3040.

- [28] B. Allen and E. P. S. Shellard, *Cosmic-string evolution: A numerical simulation*, Phys. Rev. Lett. **64** (Jan, 1990) 119–122.
- [29] T. Damour and A. Vilenkin, *Gravitational wave bursts from cusps and kinks on cosmic strings*, Phys. Rev. D **64** (Aug, 2001) 064008.
- [30] A. Albrecht, R. A. Battye, and J. Robinson, *Detailed study of defect models for cosmic structure formation*, Phys. Rev. D **59** (Dec, 1998) 023508.
- [31] K. Horiguchi, K. Ichiki, T. Sekiguchi, and N. Sugiyama, *Primordial magnetic fields from self-ordering scalar fields*, J. Cosmology Astropart. Phys. **4** (Apr., 2015) 7, [[arXiv:1501.0630](#)].
- [32] A. Lewis, *Observable primordial vector modes*, Phys. Rev. D **70** (Aug., 2004) 043518, [[astro-ph/0403583](#)].
- [33] K. Takahashi, K. Ichiki, H. Ohno, and H. Hanayama, *Magnetic Field Generation from Cosmological Perturbations*, Physical Review Letters **95** (Sept., 2005) 121301, [[astro-ph/0502283](#)].
- [34] K. Takahashi, K. Ichiki, H. Ohno, H. Hanayama, and N. Sugiyama, *Generation of magnetic field from cosmological perturbations*, ArXiv Astrophysics e-prints (Jan., 2006) [[astro-ph/0601243](#)].
- [35] K. Ichiki, K. Takahashi, and N. Sugiyama, *Constraint on the primordial vector mode and its magnetic field generation from seven-year wilkinson microwave anisotropy probe observations*, Phys. Rev. D **85** (Feb, 2012) 043009.
- [36] K. Ichiki, K. Takahashi, N. Sugiyama, H. Hanayama, and H. Ohno, *Magnetic Field Spectrum at Cosmological Recombination*, ArXiv Astrophysics e-prints (Jan., 2007) [[astro-ph/0701329](#)].
- [37] S. Saga, K. Ichiki, K. Takahashi, and N. Sugiyama, *Magnetic field spectrum at cosmological recombination revisited*, Phys. Rev. D **91** (June, 2015) 123510, [[arXiv:1504.0379](#)].
- [38] S. Saga, M. Shiraishi, K. Ichiki, and N. Sugiyama, *Generation of magnetic fields in Einstein-aether gravity*, Phys. Rev. D **87** (May, 2013) 104025, [[arXiv:1302.4189](#)].
- [39] W. Hu and N. Sugiyama, *Anisotropies in the cosmic microwave background: an analytic approach*, ApJ **444** (May, 1995) 489–506, [[astro-ph/9407093](#)].
- [40] K. Ichiki, K. Takahashi, and N. Sugiyama, *Constraint on the primordial vector mode and its magnetic field generation from seven-year Wilkinson Microwave Anisotropy Probe observations*, Phys. Rev. D **85** (Feb., 2012) 043009, [[arXiv:1112.4705](#)].
- [41] M. A. Latif, D. R. G. Schleicher, and W. Schmidt, *Magnetic fields during the formation of supermassive black holes*, MNRAS **440** (May, 2014) 1551–1561, [[arXiv:1310.3680](#)].
- [42] T. Venumadhav, A. Oklopcic, V. Gluscevic, A. Mishra, and C. M. Hirata, *A new probe of magnetic fields in the pre-reionization epoch: I. Formalism*, ArXiv e-prints (Oct., 2014) [[arXiv:1410.2250](#)].